Proceedings of the 9th International Conference on Structural Dynamics, EURODYN 2014
Porto, Portugal, 30 June - 2 July 2014
A. Cunha, E. Caetano, P. Ribeiro, G. Müller (eds.)
ISSN: 2311-9020; ISBN: 978-972-752-165-4

Prediction of macroscopic mechanical properties of a polycrystalline microbeam subjected to material uncertainties

Vincent Lucas[1], Ling Wu[1], Maarten Arnst[1], Jean-Claude Golinval[1], Stéphane Paquay[2], Van-Dung Nguyen[1], Ludovic Noels[1]
[1]Department of Aeronautic and Mechanical Eng., University of Liege, Chemin des Chevreuils 1, B-4000 Liege, Belgium
[2]Open-engineering SA, Rue des Chasseurs-Ardennais, B-4031 Liege(Angleur), Belgium
email: vincent.lucas@ulg.ac.be

ABSTRACT: The first resonance frequency is a key performance characteristic of MEMS vibrometers. In batch fabrication, this first resonance frequency can exhibit scatter owing to various sources of manufacturing variability involved in the fabrication process. The aim of this work is to develop a stochastic multiscale model for predicting the first resonance frequency of MEMS microbeams constituted of polycrystals while accounting for the uncertainties in the microstructure due to the grain orientations. At the finest scale, we model the microstructure of polycrystaline materials using a random Voronoï tessellation, each grain being assigned a random orientation. Then, we apply a computational homogenization procedure on statistical volume elements to obtain a stochastic characterization of the elasticity tensor at the second scale of interest, the meso-scale. In the future, using a stochastic finite element method, we will propagate these meso-scale uncertainties to the first resonance frequency at the coarser scale.

KEY WORDS: MEMS; Stochastic homogenization; Micro-beam resonance frequency.

1 INTRODUCTION

Microelectromechanical systems (MEMS) are microsystems made of at least one mechanical part. They are present in a wide variety of fields, including aeronautics, automobile, or medicine (e.g. heart catheter as blood pressure sensors) and their use is growing fast. Predicting precisely one or more mechanical properties is of major interest for some applications. However, a scatter between a predicted mechanical property and manufactured MEMS can be observed. This scatter results from the uncertainties involved in the manufacturing process.

These uncertainties can be of different natures. Two different MEMS will have different microstructures (grain sizes, grain orientations, surface profiles…). For a sufficiently large macroscopic scale, such randomness is negligible. However, for MEMS, the dimensions are comparable with the microstructure of materials. Thus the influence of the microstructure may not be negligible anymore.

The case study in this work is a clamped-free microbeam used for gyroscopes. For MEMS gyroscopes, structural dynamics may be of major importance. Interesting macroscopic quantities for designers are the resonance frequency of the first mode or the quality factor. The microbeam is made of polysilicon. As the properties of Silicon crystals are anisotropic, a first source of uncertainty is the grain orientation (other sources will be considered in a future work). The purpose of this work is the prediction of the macroscopic resonance frequency of the first mode of a microbeam from a random distribution of grain orientation at the microscopic scale.

The resonance frequency can be predicted by using a 3-scale stochastic model. This is necessary since modeling each grain for the whole beam is computationally too heavy. The 3 scales are the following ones:

- The micro-scale or the grain scale is the smallest scale of this model. It models each grain with its particular elasticity tensor which depends on the orientation of the grain.
- The meso-scale is the intermediate scale. It is the scale over which the material properties of the grain are homogenized.
- The macro-scale is the whole microbeam over which the resonance frequency is sought, using homogenized material properties at the meso-scale.

The link between these 3 scales is depicted in Figure 1.

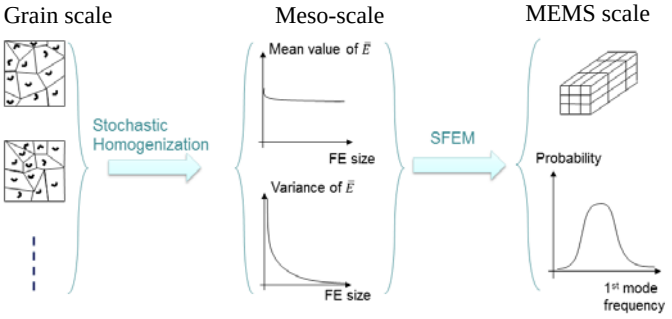

Figure 1- The 3-scale procedure

Samples of the microstructure can be generated with a random orientation for each silicon grain. They are referred to as the Statistical Volume Elements (SVE). A Monte-Carlo procedure along with a homogenization technique permits to estimate a distribution of the material properties at the meso-scale, as proposed in [1,2,3]. However computational homogenization is used here, based on [4,5,6] (see section 2.3) as it is more efficient although it requires the stiffness matrix of the microstructure. The support of the distribution can be bounded (from below and above) to match better the

observed behavior of the material. The bounds' information can be added with the maximum entropy principle (MaxEnt) [7]. The final objective of this step is to be able to generate samples of the elasticity tensor that would mimic the microstructure randomness.

Once the distribution of the elasticity tensor is obtained at the meso-scale, the uncertainties can be propagated up to the macro-scale. A deterministic finite element method can be used in the frame of a Monte-Carlo procedure. Other methods can be considered to improve the computational efficiency. Polynomial chaos expansion can be considered [8], [9]. Stochastic Finite Element methods exist, such as spectral stochastic finite element [10]. The Perturbation approach can also be used. It gives a solution at a low computational cost, even though it may lack accuracy [11], [12], [13]. Finally, the Perturbation Stochastic Finite Element Method (PSFEM) considers a Taylor expansion around the mean to determine the output distribution. This meso-macro procedure will be investigated in the future.

The sections that follow focus on the microscopic part. The material, polysilicon, is first described. The homogenization procedure is then discussed. The last section derives the distribution of the material property at an intermediate scale: the meso-scale. From samples of the microstructure, distributions of the homogenized property can be constructed.

2 THE MICROSCOPIC PART

2.1 Silicon

Silicon is the most common material in microelectromechanical systems. It is an aggregate of cubic crystalline materials. The properties of a silicon grain depend on its orientation with respect to the crystal lattice. What follows here is based on [14]. The notation (hkl) represents a plane with the integers h, k, and l being the Miller indices. $[hkl]$ represents a direction (in the basis of the direct lattice vectors).

In the [100], [010] and [001] directions, the same Young modulus is seen: 130 GPa, the minimum value for silicon. The maximum value of the Young modulus is obtained in the [111] direction: 188 GPa. The range of possible values for Poisson's ratio is between 0.048 and 0.40. The behavior of the Young modulus and the Poisson ratio is depicted in Figure 2 in the plane (100).

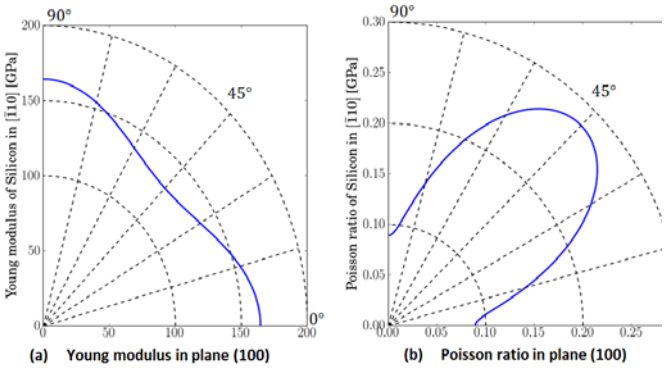

Figure 2 - Silicon material properties based on [14]

Based on [14], which uses Hall measurements [15], Table 1 contains the different properties of Silicon. The x, y and z axes are aligned with the [100], [010] and [001] directions. E stands for the Young modulus while v and G correspond respectively to the Poisson ratio and the shear modulus. The parameters c_{ab} are the (a, b) elements of the matrix Voigt notation of the fourth order elasticity tensor $\mathbb{C}$.

Table 1. Measured mechanical properties

Parameter	Hall meas.
E_x [GPa]	130
v_{xy}[-]	0.28
G_{xy} [GPa]	79.6
c_{11} [GPa]	165.6
c_{12} [GPa]	63.9
c_{44} [GPa]	79.5

2.2 Homogenization: overview

Let us consider the micro to meso part: the homogenization of a volume element of the microbeam is sought. A portion of the material taken into consideration can be named a volume element. An example of a FE model, obtained with *gmsh*, can be seen in Figure 3. When this volume is large enough to have accurate, deterministic homogenization, it is called a representative volume element (RVE). The material properties can be extracted by applying suitable boundary conditions on the FE model. The Hill-Mandel condition must be verified [4,5,6] as it will be discussed later on. The homogenized computed property is called effective and does not depend on the boundary condition. If the volume element is too small to be representative, the homogenization possesses a random nature. It is a statistical volume element (SVE). The homogenized computed property is called apparent. The apparent properties of a SVE depend on the boundary condition.

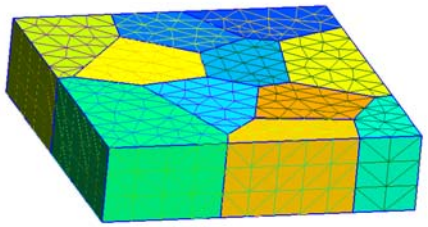

Figure 3 - A sample of the microstructure

At first, let us consider a RVE. The volume average $< a_m >$ of a_m over the volume V is defined as

$$< a_m >= \frac{1}{V}\int_{\mathrm{V}} a_m(\boldsymbol{x})dV$$

The subscript m will refer to the microstructure while the subscript M will refer to the homogenized case over the volume element. V and Γ are respectively the volume and boundary while $\boldsymbol{x}$ is the position vector. An effective elasticity tensor $\mathbb{C}_M^{eff}$ can be defined over an RVE. As said earlier, it is independent of the boundary conditions and thus unique for elastic material. $\mathbb{C}_M^{eff}$ can be defined through the relationship between the averaged stress tensor $< \boldsymbol{\sigma}_m >$ and the averaged strain tensor $< \boldsymbol{\varepsilon_m} >$ [16]:

$$< \boldsymbol{\sigma_m} >= \mathbb{C}^{eff} : < \boldsymbol{\varepsilon_m} > \quad (1)$$

If a' is the fluctuation of a_m around its volume average$< a_m >$, then the following can be written ([16]):

$$\mathbb{C}_M^{eff} : < \boldsymbol{\varepsilon_m} >=< \mathbb{C}_m >: < \boldsymbol{\varepsilon_m} > +< \mathbb{C}'_m : \boldsymbol{\varepsilon_m}' >$$

Thus $\mathbb{C}_M^{eff}$ usually differs from $< \mathbb{C}_m >$. The latter is the approximate solution proposed by Voigt: the homogenized elasticity tensor is approximated by its average local value. As said by Hill, that solution is an upper bound for $\mathbb{C}_M^{eff}$. It is named the Hill-Voigt bound.

The same reasoning can be done with the compliance tensor. $< \mathbb{S}_m >^{-1}$ is then a lower bound for the effective elasticity tensor. It is named the Hill-Reuss bound.

Bounds will be important in this section. How can we define ordering between 2 tensors? A tensor $\boldsymbol{A}$ is (strictly) greater than a tensor $\boldsymbol{B}$ if their difference is positive semidefinite (positive definite).

$$\boldsymbol{A} > (\geq) \boldsymbol{B} \text{ iif } \boldsymbol{A} - \boldsymbol{B} \text{ is positive (semi)definite}$$

Let us define the boundary conditions that respect the Hill-Mandel principle:

- Kinematic Uniform Boundary Condition (KUBC)
- Static Uniform Boundary Condition (SUBC)
- Mixed Boundary Condition (MBC)
- Periodic Boundary Condition (PBC)

The independence of an RVE with respect to the boundary condition, when performing homogenization, can be used to define the concept of RVE. A volume element is said to be representative when the homogenized values obtained with KUBC and SUBC coincide [5]. If it is not the case, the volume element is too small to be representative and is stated statistical (SVE). KUBC and SUBC are two extreme boundary conditions (BC).

While the mixed and the periodic cases are estimates of the effective elasticity tensor, the uniform displacement (KUBC) overestimates the elasticity tensor while the static uniform BC underestimates it. For a SVE, the KUBC solution is an upper bound for the elasticity tensor while the SUBC case is a lower bound. A range of elasticity tensors is possible and one may talk about apparent properties. This can be seen in Figure 4. The most accurate estimate of the effective property is the PBC case: it converges in a faster way with respect to the size of the volume element. On the other hand, the mixed case is easier to implement.

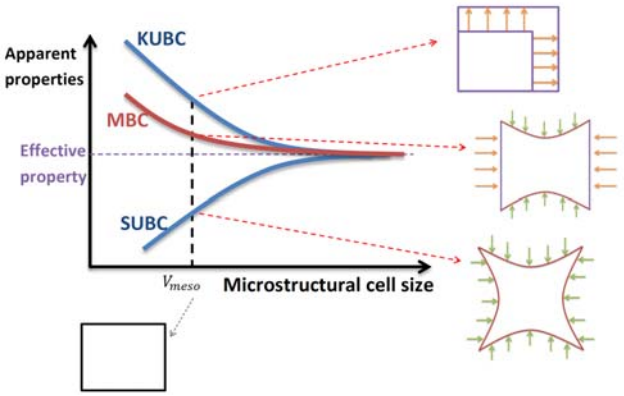

Figure 4 - Young modulus for different SVE under different BCs

2.3 *Homogenization: implementation*

This paper is strongly influenced by the work of both [1] and [2]. In these works, the elasticity tensor at the meso-scale is computed with uniform displacement BC (KUBC), uniform traction BC (SUBC) as well as mixed boundary condition (MBC) along with Huet's partition theorem [16]. The latter is used to compute the apparent elasticity tensor. The volume averages of both the deformation and the stress are required, with the help of a minimization procedure. When one has access to the stiffness matrix of the FE model, there is another way to get the elasticity tensor: computational homogenization. It is more efficient than [1,2] but requires the stiffness matrix.

Here the work done in [4,5], dealing with computational homogenization, is used. The macro stress tensors $\boldsymbol{\sigma}_M$ and the macro strain tensor $\boldsymbol{\varepsilon}_M$ are defined from the volume averages of their corresponding micro tensors:

$$\begin{cases} \boldsymbol{\sigma}_M =< \boldsymbol{\sigma}_m >= \frac{1}{V}\int_V \boldsymbol{\sigma}_m dV \\ \boldsymbol{\varepsilon}_M =< \boldsymbol{\varepsilon}_m >= \frac{1}{V}\int_V \boldsymbol{\varepsilon}_m dV \end{cases} \quad (2)$$

The Hill-Mandel principle implies the equality of the internal energy at both scales yielding:

$$\boldsymbol{\sigma}_M : \boldsymbol{\varepsilon}_M = \frac{1}{V}\int_V \boldsymbol{\sigma}_m : \boldsymbol{\varepsilon}_m dV \quad (3)$$

In the absence of body forces it can be shown [6] that this relation reduces to

$$0 = \int_\Gamma (\boldsymbol{t}_m - \boldsymbol{\sigma}_M \cdot \boldsymbol{n}_m) \cdot (\boldsymbol{u}_m - \boldsymbol{\varepsilon}_M \cdot \boldsymbol{x}) d\Gamma \quad (4)$$

where $\boldsymbol{n}_m$ is the normal to the boundary Γ of the micro-volume, $\boldsymbol{t}_m = \boldsymbol{\sigma}_m \cdot \boldsymbol{n}_m$ is the surface traction, and where $\boldsymbol{u}_m$ is the micro-displacement field. To introduce consistent boundary conditions at the micro-scale, the displacement field $\boldsymbol{u}_m$ can be decomposed into an average $\bar{\boldsymbol{u}}_m = \boldsymbol{\varepsilon}_M \cdot \boldsymbol{x}$ and into a fluctuation field $\boldsymbol{u}'_m$ so that

$$\boldsymbol{u}_m = \bar{\boldsymbol{u}}_m + \boldsymbol{u}'_m = \boldsymbol{\varepsilon}_M \cdot \boldsymbol{x} + \boldsymbol{u}'_m$$

The fluctuation $\boldsymbol{u}'_m$ comes from the resolution of the micro-scale problem. As seen in [6], the Hill-Mandel principle (4) becomes:

$$\int_\Gamma \boldsymbol{t}_m \cdot \boldsymbol{u}'_m \, d\Gamma = 0 \quad (5)$$

This condition is satisfied for each of the previously defined boundary conditions, which are now specified.

- No microstructural fluctuations over the whole volume element:

$$\boldsymbol{u}_m = \boldsymbol{\varepsilon}_M \cdot \boldsymbol{x}, \ \forall \boldsymbol{x} \in V$$

  This case is the Voigt assumption.

- No microstructural fluctuations over the boundary:

$$\boldsymbol{u}_m = \boldsymbol{\varepsilon}_M \cdot \boldsymbol{x}, \ \forall \boldsymbol{x} \in \Gamma \quad (6)$$

  It is the kinematic uniform case (KUBC).

- Periodicity can also be enforced with volume elements of periodic geometry. Therefore the microstructural fluctuations of an edge $\boldsymbol{u}'^{+}_m$ are equal to the fluctuations of the opposing edge $\boldsymbol{u}'^{-}_m$.

- The whole boundary integral (4) can vanish as a whole. It is the weakest possible constraint. It is named the minimal kinematic boundary conditions and it can be written as :

$$\boldsymbol{t}_m = \boldsymbol{\sigma}_M \cdot \boldsymbol{n}_m, \ \forall \boldsymbol{x} \in \Gamma$$

  This corresponds to a uniform traction over the boundary, or SUBC and can be simulated by considering

$$\int_{\Gamma^\pm} (\boldsymbol{u}'_m \otimes \boldsymbol{n}_m) \, d\Gamma = 0 \quad (7)$$

  on the opposite RVE faces $\Gamma^\pm$ as proved in [5]. Note that this equation can be enforced by constraining the displacement of the volume faces.

- The mixed case is a combination of KUBC and SUBC in the x and y directions. Equation (6) or (7) is used, depending on the boundary.

- Finally, the equality between the stresses at the micro and macro scales over the whole volume corresponds to the Reuss assumption:

$$\boldsymbol{\sigma}_m = \boldsymbol{\sigma}_M \ , \ \forall \boldsymbol{x} \in V \quad (8)$$

Let us now define a way to compute the elasticity tensor. More details can be found in [5,6]. At first, the macroscopic stress tensor can be written as:

$$\boldsymbol{\sigma}_M = \frac{1}{V} \int_\Gamma \boldsymbol{t} \otimes \boldsymbol{x} d\Gamma \quad (9)$$

When applicable boundary conditions, in the Hill-Mandel sense, are considered, there are N_{nd} nodes with prescribed displacements, N_{nd} depending on the type of boundary condition. With $\boldsymbol{x}^p$ being their position vector in the deformed state, equation (9) can be rewritten as:

$$\boldsymbol{\sigma}_M = \frac{1}{V} \sum_{p=1}^{N_{nd}} \boldsymbol{f}^p \otimes \boldsymbol{x}^p \quad (10)$$

where $\boldsymbol{f}^p$ corresponds to the resulting external nodal forces at the prescribed nodes. In linear elasticity, the equilibrium between external and internal forces can be written the following way:

$$\sum_q \boldsymbol{K}_M^{pq} . \boldsymbol{u}^q = \boldsymbol{f}^p \quad (11)$$

where p and q corresponds to the different N_{nd} prescribed nodes, and where $\boldsymbol{K}_M^{pq}$ is obtained thanks to a condensation of the internal nodes [5]. This condensation depends on which boundary condition is used.

Including (11) in (10) results in:

$$\boldsymbol{\sigma}_M = \frac{1}{V} \sum_p \sum_q \left(\boldsymbol{K}_M^{pq} \boldsymbol{u}^q \right) \otimes \boldsymbol{x}^p$$

or again, as the displacement of the constraint nodes directly comes from the deformation tensor:

$$\boldsymbol{\sigma}_M = \frac{1}{V} \sum_p \sum_q \boldsymbol{x}^p \otimes \boldsymbol{K}_M^{pq} \otimes \boldsymbol{x}^q : \boldsymbol{\varepsilon}_M$$

The homogenized elasticity tensor $\mathbb{C}_M$ can be defined as:

$$\boldsymbol{\sigma}_M = \mathbb{C}_M : \boldsymbol{\varepsilon}_M \quad (12)$$

and thus, one can write:

$$\mathbb{C}_M = \frac{1}{V} \sum_p \sum_q \boldsymbol{x}^p \otimes \boldsymbol{K}_M^{pq} \otimes \boldsymbol{x}^q \quad (13)$$

2.4 Extraction of the mesoscopic properties

Now the elasticity tensor of a volume element will be computed. The size, number of grains and number of samples for different considered SVE are given in Table 2.

Table 2. Different SVEs realizations

Case	xy area[μm^2]	Number of grains	Number of samples
1	0.03	2	400
2	0.088	6	300
3	0.164	11	150
4	0.224	15	100
5	0.282	19	100

The different SVE can be seen in Figure 5.

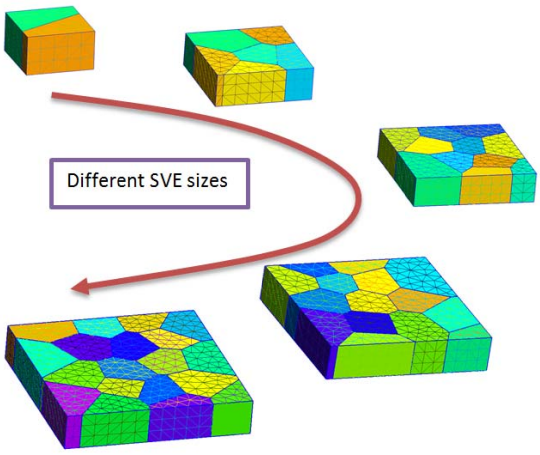

Figure 5 - the different SVEs

The Voronoï tessellation for one SVE size is deterministic. Only the orientation of each grain is random. A set of orientations, one for each grain, defines a realization $\boldsymbol{\theta}_k$ of the microstructure. $\boldsymbol{\theta}_k$ represents the randomness of each sample k among the N_s realizations of the microstructure. There is no preferred direction. The stiffness matrix $\boldsymbol{K}(\boldsymbol{\theta}_k)$ of the microstructure, when applying mixed BC, is used to compute the elasticity tensor. The results obtained from the Monte-Carlo simulations (N_s realizations) are represented in Figure 6 and Figure 7.

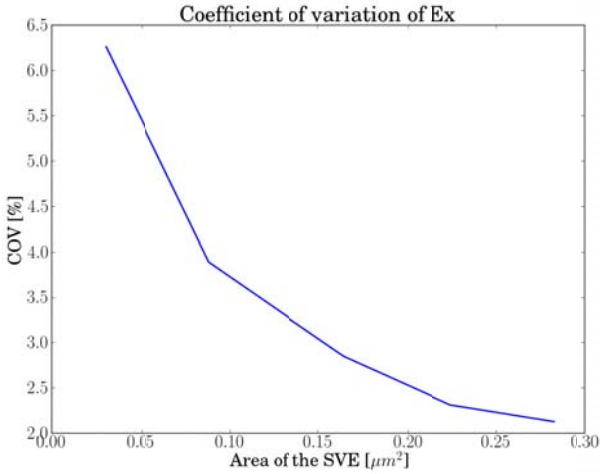

Figure 6 - Coefficient of variation of E_x

In Figure 6, the coefficient of variation(COV) is depicted. The COV is linked to the standard deviation and the mean: $COV = \sigma/\mu$. As expected, increasing the size of the volume element decreases the coefficient of variation of the Young modulus (from ≈ 6% to ≈ 2%).

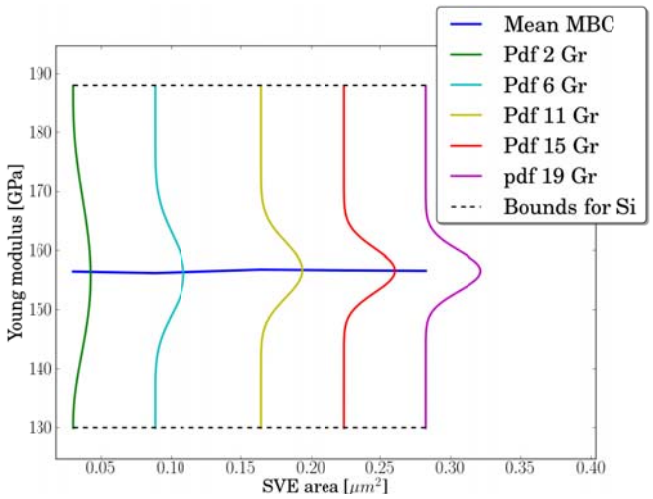

Figure 7 - E_x for different boundary conditions

In Figure 7, one can see the mean Young modulus in the x direction: it does not vary much with the SVE size. The bounds for a single crystal Silicon are 130 GPa and 188 GPa as presented in Figure 7. Whatever the size of the SVE (and so the number of grains), there is a chance that each grain is orientated in one of these extreme case. Thus having a SVE of 130 GPa or 180 GPa is always possible. However it is less likely with a growing number of grains. It is seen in Figure 7: the colored curves are the probability density function of the Young modulus in the x direction based on a beta distribution, directly obtained from the Monte-Carlo simulations (the bounds being those of a single Silicon crystal). The probability to be close to the silicon bounds decreases drastically as the size of the SVE grows.

3 THE MESOSCOPIC PROPERTIES

In the previous section, the generation of a sample of the microstructure was described. The randomness was expressed through grains of random orientation. Different boundary conditions can be applied over this microstructure. Furthermore the homogenized elasticity tensor of this sample can be computed.

In this section, with the aim of predicting stochastic macro properties, the use of the mesoscopic properties in a FE context is expanded.

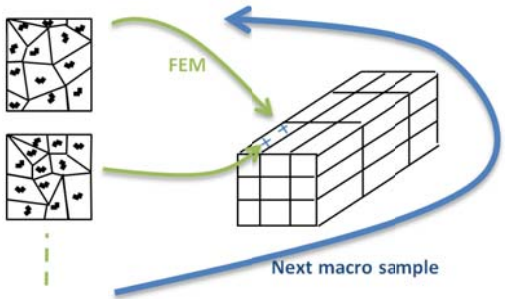

Figure 8 - Procedure without generator

Say we want to perform a Monte-Carlo simulation to get the distribution of the resonance frequency f_1 of a microbeam. To achieve this, N_{sim} samples of f_1 are required and they can be computed thanks to a Finite Element method. A sample for the elasticity tensor is required for each Gauss point of this FE model. If we have N_{Gs} Gauss points and if we want N_{sim} simulations of the FE model, then we need $N_{Gs} \cdot N_{sim}$ samples of the elasticity tensor. Furthermore, in order to perform another simulation with a different set of samples, one needs to compute all the micro parts again. This process is depicted in Figure 8: at each Gauss point, a new set of the microstructures is required. Evidently, it is less costly to compute enough samples of the microstructure to capture its statistical behavior and to use a generator. Correlation between different Gauss points can also be added. This solution is represented in Figure 9.

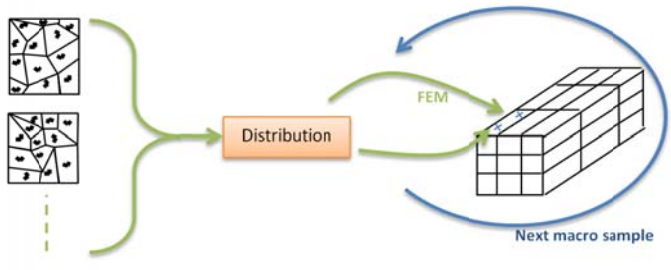

Figure 9 - Procedure with generator

To apply this solution, we first need to define a distribution of the material property of interest and to compute its parameters. Then samples need to be generated according to this distribution.

The mixed boundary condition provides an estimation of the elasticity tensor. Therefore we can estimate the mean and the variance of material properties given by the elasticity tensor as the Young modulus. A gamma distribution can be derived from this information and samples can be generated from various libraries.

Also one may want to generate the whole elasticity tensor. Things are however more difficult when working with tensors, especially when lower and upper bounds constrain the desired tensor. Such bounds are present in this case with the help of the KUBC and SUBC [1,2,3].

3.1 1D case for E_x

The distribution considered here is based on the samples of E_x. Furthermore, it possesses a lower bound E_x^l as well as an upper bound E_x^u. For a constant SVE size, samples of bounds can be obtained with KUBC and SUBC. As it is a set of real numbers, the bounds are simply the maximum (minimum) of E_x^{KUBC} (E_x^{SUBC}). A mean $\bar{E}_x$ and a variance $\sigma_{E_x}^2$ can be estimated from the samples of E_x^{PBC} or E_x^{MBC}. Here the mixed case is used.

The following linear change of variable can be made:

$$u = \frac{E_x - E_x^l}{E_x^u - E_x^l} \tag{14}$$

It is assumed that u follows a beta based distribution between 0 and 1.The parameters of the distribution α and β are:

$$\alpha = \frac{\bar{u}^2(1-\bar{u})}{\sigma_u^2} - \bar{u}$$
$$\beta = \frac{\bar{u}(1-\bar{u})^2}{\sigma_u^2} + \bar{u} - 1$$

The samples of E_x are used to compute $\bar{u}$ and σ_u, respectively the mean value and the standard deviation of u. The distributions obtained with different sizes of the volume element can be seen in Figure 10. This set of curves is similar to the set which was directly obtained from the probability density function of the Young modulus in the x direction based on a beta distribution, directly obtained from the Monte-Carlo simulations reported in Figure 7. The main difference is that in the new distribution the bounds narrow the Young modulus range with an increasing size of the volume element.

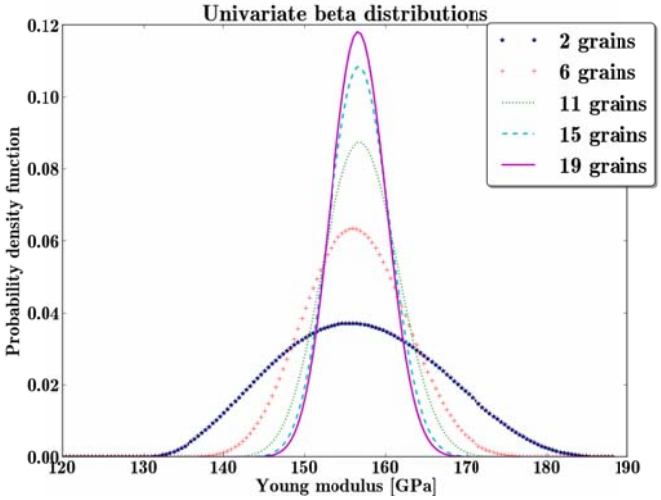

Figure 10 - Univariate beta distributions of different SVE sizes

3.2 3D case

In this section we deal with the distribution of the whole elasticity tensor $\mathbb{C}_M$. The problem is simplified with the help of the Voigt notation: from a fourth order $\mathbb{C}_M$, we can define a second order matrix $\boldsymbol{C}$ (we omit the subscript M for clarity).

3.2.1 Absolute bounds

The first problem we face is the definition of 2 absolute bounds $\boldsymbol{C}_u$ and $\boldsymbol{C}_l$. Samples of bounds can be computed with the different boundary conditions. What is needed is one upper bound, above each sample, and one lower bound, below each sample. This is not as easy as in 1D: tensors face Loewner partial ordering. The solution is not the supremum and the infimum based on a set of realizations.

For each microstructure, we know that the elasticity tensor is below the KUBC case. Therefore $\boldsymbol{C}_u$ is defined as a tensor higher than each KUBC case. In order to use as much information as we can, it will also be the closest tensor to each of them. The same reasoning can be performed for $\boldsymbol{C}_l$ and the SUBC case.

In [1] and [2], the absolute bounds are defined the following way:

$$\boldsymbol{C}_l = \arg\min_{\boldsymbol{C}\in\boldsymbol{C}_{ad}^l} \sum_{k=1}^{N_s} \|\boldsymbol{C}^{SUBC}(\boldsymbol{\theta}_k) - \boldsymbol{C}\|_F$$

$$\boldsymbol{C}_u = \arg\min_{\boldsymbol{C}\in\boldsymbol{C}_{ad}^u} \sum_{k=1}^{N_s} \|\boldsymbol{C} - \boldsymbol{C}^{KUBC}(\boldsymbol{\theta}_k)\|_F$$

with $\|a\|_F$ being the Frobenius norm of a. These two equations ensure that the absolute bounds are close to the sampled bounds. Both sets $\boldsymbol{C}_{ad}^l$ and $\boldsymbol{C}_{ad}^u$ ensure that $\boldsymbol{C}_l$ and $\boldsymbol{C}_u$ are bounds for each sampled microstructure:

$$\boldsymbol{C}_{ad}^l = \{\boldsymbol{C} \in \mathbb{M}_n^+(\mathbb{R}) | \boldsymbol{C} < \boldsymbol{C}^{SUBC}(\boldsymbol{\theta}_k), k = 1, \dots, N_s\}$$
$$\boldsymbol{C}_{ad}^u = \{\boldsymbol{C} \in \mathbb{M}_n^+(\mathbb{R}) | \boldsymbol{C}^{SUBC}(\boldsymbol{\theta}_k) < \boldsymbol{C}, k = 1, \dots, N_s\}$$

To reduce the size of this problem, one can assume that the bounds are isotropic or orthotropic. The problem remaining is an optimization procedure of dimension 2 (isotropic assumption) or 3 (orthotropic assumption).

3.2.2 Maximum entropy

For now, we have samples of the elasticity tensor and two absolute bounds. What remains to be defined at the meso-scale is the distribution of the elasticity tensor as well as to be able to generate samples from this distribution. To achieve this, the maximum entropy principle can be used.

As recalled in [1], *the maximum entropy principle consists of maximizing the measure of entropy S(p) under a set of constraints encompassing the available information.* The measure of information entropy can be defined as:

$$S(\mathbb{P}) = -\int_{\mathbb{M}_n^+(\mathbb{R})} \mathbb{P}(\boldsymbol{C}) \ln\big(\mathbb{P}(\boldsymbol{C})\big)\, d\boldsymbol{C}$$

where, $d\boldsymbol{C}_{ij}$ being Lebesgue measure on $\mathbb{R}$, the measure $d\boldsymbol{C}$ is:

$$d\boldsymbol{C} = 2^{\frac{n(n-1)}{4}} \prod_{1\le i\le j\le n} d\boldsymbol{C}_{ij}$$

To define a probability density function for $\boldsymbol{C}$, one step remains: the definition of the constraints. It can be done in various ways. In [3], they are defined as:

$$\begin{cases} \int_{\boldsymbol{C}} \mathbb{P}(\boldsymbol{C}) d\boldsymbol{C} = 1 & (15) \\ \mathbb{E}[\ln(\det(\boldsymbol{C}_u - \boldsymbol{C}))] = c_u & (16) \\ \mathbb{E}[\ln(\det(\boldsymbol{C} - \boldsymbol{C}_l))] = c_l & (17) \\ \mathbb{E}[\boldsymbol{C}] = \overline{\boldsymbol{C}} & (18) \end{cases}$$

The scalar parameters c_u and c_l can be computed from the generated samples as well as the matrix mean $\overline{\boldsymbol{C}}$.

As can be seen in [1], maximizing entropy under constraints (15)-(18) gives a generalized matrix variate Kummer-Beta distribution for the probability density function of the elasticity tensor:

$$\mathbb{P}(\boldsymbol{C}) = \mathbb{I}(\boldsymbol{C}) c_0 \det(\boldsymbol{C} - \boldsymbol{C}_l)^{\lambda_l} \det(\boldsymbol{C}_u - \boldsymbol{C})^{\lambda_u}\, etr(-\boldsymbol{\Lambda}_C \mathbf{C})$$

where $etr(\boldsymbol{X}) = \exp[tr(\boldsymbol{X})]$ and c_0 is the normalization constant based on λ_0: $c_0 = \exp(\lambda_0)$. The 3 scalar parameters λ_0, λ_u and λ_l and the matrix parameter $\boldsymbol{\Lambda}_C$ are the Lagrange multipliers of constraints (15) to (18) respectively. Each of them can be computed following [3]. More information concerning matrix variate Kummer Beta distribution can be found in [17]. How to generate matrix variate Kummer Beta distribution is explained in [3]. Computing the parameters of this distribution involves non-linear optimization and matrix hypergeometric functions. Generating matrices from this distribution implies slice sampling strategies, Gibbs sampling or Markov-chain Monte-Carlo methods.

An alternative was proposed in [1] and [2]: thanks to a change of variable, only the generation of Gaussian and Gamma random numbers is required. The change of variable is the following:

$$\boldsymbol{N} = (\boldsymbol{C} - \boldsymbol{C}_l)^{-1} - (\boldsymbol{C}_u - \boldsymbol{C}_l)^{-1} \qquad (19)$$

This change of variable is powerful because, when the elasticity tensor $\boldsymbol{C}$ is in between its two bounds, $\boldsymbol{N}$ is positive definite. Ensuring the constraint:

$$\boldsymbol{C}_l < \boldsymbol{C} < \boldsymbol{C}_u$$

is thus equivalent to:

$$\mathbf{0} < \boldsymbol{N}$$

The probability density function of $\boldsymbol{N}$ is then (see [18]):

$$\mathbb{P}(\boldsymbol{N}) = \mathbb{I}_{\mathbb{M}_n^+(\mathbb{R})}(\boldsymbol{N}) c_0' \det(\boldsymbol{N})^{\lambda - 1}\, etr(-\boldsymbol{\Lambda}_N \boldsymbol{N})$$

It is the maximum-entropy probability distribution for positive-definite matrices [7]. Replacing $\boldsymbol{N}$ by its elasticity tensor counterpart using equation (19) gives the probability density function of $\boldsymbol{C}$ with the use of the random matrix $\boldsymbol{N}$. c_0' is the new normalization constant while λ and $\boldsymbol{\Lambda}_N$ are the Lagrange multipliers of the problem defining random matrix $\boldsymbol{N}$.

The determination of the parameters of the distribution and the generation of its random matrices are made easier using random matrix $\boldsymbol{N}$ thanks to Soize work on positive-definite random matrices [7,18,19,20].

Using the random matrix $\boldsymbol{N}$ also possesses drawbacks. Although the same amount of information is used, more flexibility can be obtained with the matrix-variate Kummer-beta distribution (more parameters are present as more constraints are enforced). Furthermore, at least in a direct way, constraining the mean value of $\boldsymbol{C}$ is not possible with the use of the random matrix $\boldsymbol{N}$ (non-linear transformation from $\boldsymbol{C}$ to $\boldsymbol{N}$).

A third possibility is the random matrix $\boldsymbol{N}'$ which is defined as:

$$\boldsymbol{N}' = \boldsymbol{C} - \boldsymbol{C}_l$$

4 CONCLUSION

This work described a way to propagate uncertainties from a random microstructure up to the meso-scale. The material considered was polysilicon, an anisotropic material, in linear elasticity. The randomness was expressed through a random orientation of the different grains of the microstructure. Computational homogenization was used to define the homogenized elasticity tensor. With the help of different boundary conditions, realizations of the elasticity tensor could be obtained along with samples of bounds. This information can be brought in a matrix-variate Kummer-Beta distribution. The latter can be replaced by a different distribution, easier to generate, with the help of an efficient change of variable.

The objective of this work is to propagate the uncertainties from the microstructure up to a macro-scale quantity. From the distribution of the homogenized elasticity tensor at the meso-scale, the computation of the uncertainties concerning a macro-scale property can be sought. This propagation will be considered in a future work. The perturbation method can provide a faster solution than Monte-Carlo based procedures.

However the main problem is to define the SVE size that would provide relevant uncertainties at macro-scale.

ACKNOWLEDGMENTS

The research has been funded by the Walloon Region under the agreement no 1117477 (CT-INT 2011-11-14) in the context of the ERA-NET MNT framework.

REFERENCES

[1] J. Guilleminot, A. Noshadravan, C. Soize and R.G. Ghanem, *A probabilistic model for bounded elasticity tensor random fields with application to polycrystalline microstructures*, Comput. Methods Appl. Mech. Engrg., Elsevier, Paris, France, 1637-1648, 2011.

[2] A. Noshadravan, R. Ghanem, J. Guilleminot, I. Atodaria and P. Peralta, *Validation of a probabilistic model for mesoscale elasticity tensor of random polycrystals*, International journal for uncertainty quantification, 73-100, 2013.

[3] S. Das and R. Ghanem, *A bounded random matrix approach for stochastic upscaling*, Society for Industrial and Applied Mathematics, 296-325, 2009.

[4] C. Miehe, A. Koch, *Computational micro-to-macro transitions of discretized microstructures undergoing small strains*. Archive of Applied Mechanics 72 (4), 300–317, 2002.

[5] V. Kouznetsova, W.A.M. Brekelmans, F.P.T. Baaijens, *An approach to micro-macro modeling of heterogeneous materials*. Computational Mechanics, 27 (1), 37–48, 2001.

[6] V.D. Nguyen, E. Bechet, C. Geuzaine and L. Noels, *Imposing periodic boundary condition on arbitrary meshes by polynomial interpolation*, Computational materials science, Elsevier, 390-406, 2012.

[7] C. Soize, *Maximum entropy approach for modeling random uncertainties in transient elastodynamics*, J. Acoust. Soc. Am., May 2001.

[8] M. Arnst and J-P. Ponthot, *An overview of non-intrusive characterization, propagation and sensitivity analysis of uncertainties in computational mechanics*, international journal for uncertainty quantification, 2013

[9] B. Debusschere, *Polynomial chaos based uncertainty propagation*, KUL Uncertainty Quantification summer school, Mai 2013.

[10] R. Ghanem and P. Spanos, *Stochastic finite elements: a spectral approach*, Springer Verlag, 1991.

[11] M. Kleiber, *The stochastic finite element method: basic perturbation technique and computer implementation*, Wiley, 1992

[12] B. Van Den Nieuwenhof and J-P. Coyette, *Modal approaches for the stochastic finite element analysis of structures with material and geometric uncertaintie*, Comput. Methods Appl. Mech. Engrg., Elsevier, pages 3706-3729, 2003.

[13] S. Lepage, *Stochastic finite element method for the modeling of thermoelastic damping in micro-resonators*, Phd thesis, University of Liege, 2007.

[14] M.A. Hopcroft, W.D. Nix, T.W. Kenny, *What is the young modulus of Silicon*, Journal of microelectromechanical systems, 229-238, April 2010.

[15] J.J. Hall, *Electronic effects in the constantsof n-type silicon*, Phys. Rev., vol. 161, no. 3, 756-761, 1967

[16] C. Huet, *Application of variational conceptsto size effects in elastic heterogeneous bodies*, J. Mech. Phys. Solids, pages 813-841, 1990.

[17] D. K. Nagar and A. K. Gupta, *Matrix-variate Kummer-Beta distribution*, J. Austral. Math. Soc., 73, 11-25, 2002.

[18] C. Soize, *Random matrix theory for modeling uncertainties in computational mechanics*, Computer methods in applied mechanics and engineering, Elsevier, 1333-1366, 2004.

[19] C. Soize, *A nonparametric model of random uncertainties on reduced matrix model in structural dynamics*, Probabilistic Engrg. Mech. 15, 277-294, 2000.

[20] C. Soize, *Non-Gaussian positive-definite matrix-valued random fields for elliptic stochastic partial differential operators*, Comput. Methods Appl. Mech. Engrg., Elsevier, 26-64, 2006.